SEY Monte Carlo modelling of conditioned Ag and Cu substrates

Christophe Inguimbert, Quentin Gibaru, Pablo Caron, Marco Angelucci, Luisa Spallino, Mohamed Belhaj, Roberto Cimino, Denis Payan

SEY Monte Carlo modelling of conditioned Ag and Cu substrates

C. Inguimbert[(1)], Q. Gibaru[(1, 2, 3)], P. Caron[(1)], M. Angelucci[(4)], L. Spallino[(4)], M. Belhaj[(1)], R. Cimino[(4)], D. Payan[(3)]

[(1)] ONERA-DESP, 2 avenue E. Belin, 31055 Toulouse, France
Email: Christophe.Inguimbert@onera.fr, Quentin.Gibaru@onera.fr, Pablo.Caron@onera.fr, Mohamed.Belhaj@onera.fr
[(2)] CEA, DAM, DIF - 91297 ARPAJON, France
[(3)] French Space Agency CNES 18 av. E. Belin, 31401 Toulouse cedex, France.
Email:Denis.Payan@cnes.fr
[(4)] LNF-INFN, Via E. Fermi 54, 00044 Frascati (Rome), Italy

INTRODUCTION

Secondary electron emission often appears as a parasitic physical process in systems that either use electrons of a few hundred eV, or that can evolve in an environment where low energy electrons are present [1]. In certain cases, by an avalanche phenomenon, electrons can multiply to a level that can disturb the functioning of sensitive equipments (multipactor) [1] or lead to catastrophic effects such as corona discharges. Multipacting is an issue for space systems that undergo electrons trapped in the earth radiation belts [2]. The satellite's power chain is particularly sensitive to this physical mechanism. In this context, the risk associated with the electron secondary emission can be mitigated by surface treatments [3] of the walls of the Radio Frequency (RF) devices. The Total Electron Emission Yield (TEY) is closely dependent to the surface state and to the nature of the coating deposited on the material. For instance, the chemical state of the surface is modified by the irradiation in a way that the TEY can be reduced. It is known that irradiations can polymerize organic molecules present at the surface of the material and fix on it a layer of graphite. Since graphite has a low emission yield, the presence of a layer of a few nanometres thick is sufficient to drive and reduce the TEY [4]. This has been shown experimentally [4], but, few numerical simulations of such behaviour have already been performed. The objective of the work presented here, is to study numerically the impact of thin carbon layers of different thicknesses, on the SEY of Ag and Cu substrates, using Monte Carlo simulations [5-[8].

MONTE CARLO TRANSPORT CODE FOR LOW ENERGY ELECTRONS

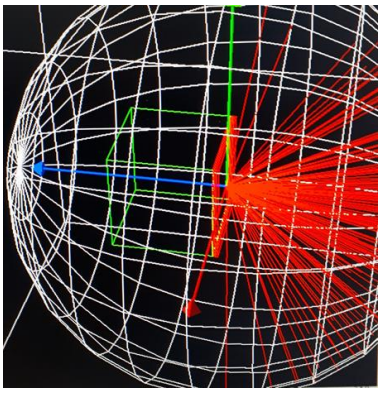

Fig. 1. Example of GEANT4 simulation, 500 eV incident electrons on a copper target. The surrounding sphere is the detector devoted to the electrons counting.

An incoming particle such as an electron impinging a material act at the atomic scale like an electromagnetic wave crossing a medium with particular dielectric properties. The polarization induced by the incident wave results in an interference phenomenon that change the phase of the wave which results in a change of the trajectory of the incident particle which can be either scattered or absorbed. The response of the medium to the external electromagnetic excitation is condensed in the complex dielectric function of the material, wich depends itself on the electric susceptibility χ:

$$\varepsilon^{-1}(\vec{k},\omega) = 1 + \frac{4\pi}{k^2}\chi(\vec{k},\omega) \quad (1)$$

Where ~~k~~ $\vec{k}$ is the wave vector of the incoming particle and ε the complex dielectric function of the material. In that sense, the dielectric theory is very effective to quantify the transport of particles at low energy in an energy domain where it is complex to get the typical response of weakly bound electrons belonging to the valence and conduction bands. The low

energy domain for electrons extends from a few eV to a few keV. It can be demonstrated that the electron/electron interaction cross sections can be deduced from the imaginary part of the inverse of the complex dielectric function. The Optical Energy Loss Function (OELF) has been exploited to derivate the interaction cross section using the Mermin's dielectric function -[5-8].

$$\frac{d\sigma}{dW} = Z_{\text{eff}}^2 \frac{m_q}{m_e \pi N a_0 T} \int_{q-}^{q+} \frac{1}{q} \text{Im}\left[-\frac{1}{\varepsilon(q,\omega)}\right] dq \qquad (2)$$

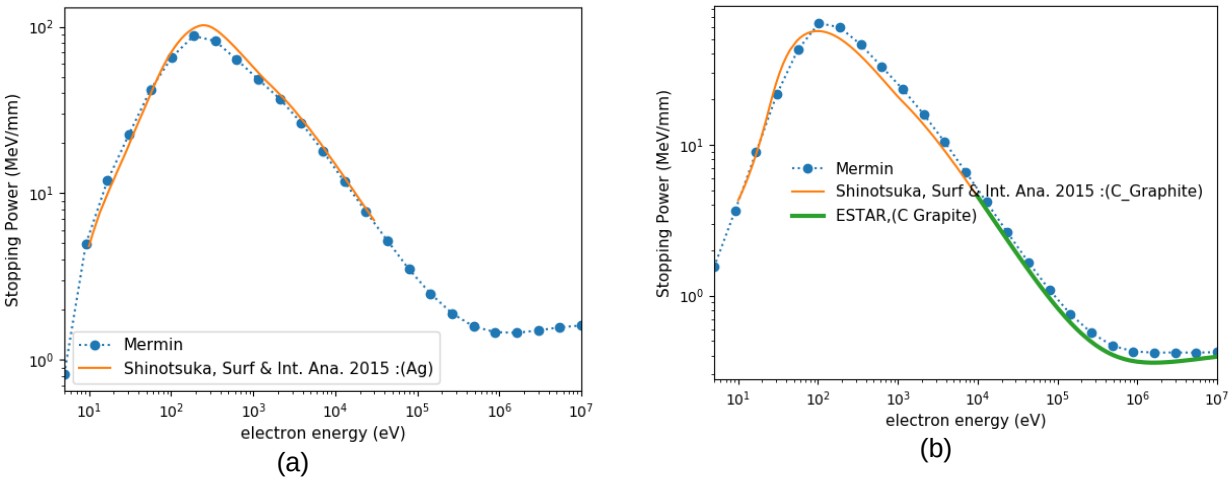

Fig. 2. Electron stopping power in silver (a) and carbon (b). Comparions is made with Shinotsuka data [9] and NIST/ESTAR model for high energy [10].

The OELF treatment has been applied for silver, copper and carbon materials for which the interaction cross sections have been calculated and validated by comparisons of the electronic stopping power of incident electrons of reference [9]. The Monte Carlo toolkit that has been developed [5-8] has been fed with these data. The elastic scattering process has been modelled using the ELSEPA code [11] that performs the relativistic (Dirac) partial-wave calculations for scattering by a local central coulombic potential [11]. These developments are now available through the GEANT4 package [12] for a list of 9 materials (C, Al, Si, Ti, Ni, Cu, Ge, Ag and W). It allows the calculation of the Secondary Electron emission Yield (SEY) of these different materials on the energy range [~eV, ~keV]. The material/material interface is treated according to a quantum reflection/refraction process that include the difference in materials work functions [5-8]. For more details about the Monte Carlo transport code readers can refer to references [5-8].
A dedicated GEANT4 application has been developed to estimate the TEY of irradiated surface. A geometry composed of a stack of 5 layers, whose thickness and material composition can be parameterized by the user, is irradiated by an incident electron beam whose incident direction can be also chosen by the user (Fig. 1). A spherical detector surrounding the irradiated volumes (Fig. 1) counts the number of electrons escaping the geometry. True Secondary Electrons Yield (SEY) is differentiated from Backscattered Emission Yield (BEY) and TEY = SEY + BEY (Total Electron Yield). The amount of real backscattered electrons is counted by default. The electrons having an energy greater than 50 eV is also estimated. The latter counting method is necessary for comparisons with experimental data that are estimated on this assumption. Depending on the case we will use one or the other of these conventions for the BEY. The corresponding BEY will then be noted BEY or BEY (>50eV).

TEY FOR SILVER AND COPPER SUBSTRATES TOPED WITH THIN GRAPHITE LAYERS

Case of silver substrate

On Fig. 3 are plotted the total emission yields (TEY), sum of secondary emission yields (SEY) and backscattered emission yields (BEY), of different geometrical configurations. The TEY is presented between 25 eV and 3 keV for different geometrical structures made of a silver substrate covered with a graphite layer of variable thickness ranging from 1 nm up to 50 nm. Pure graphite and silver TEY are also shown. These two curves border all TEY curves, they represent respectively the higher and lower limit of all the simulated TEY. TEY curves of graphite and silver have quite different shapes despite their similarity. These yield curves, present a classical maximum, centered around a few hundred eV, and

border by the two cross-over points where the TEY becomes equal to 1. The carbon TEY curve is narrower than the one of silver. Exceeding the unit is critical in terms of secondary emission, since it allows the multiplication of electrons by promoting an avalanche phenomenon. We can clearly see that the second cross-over point for silver is around a few keV while it is only ~500 eV for carbon. The deposition of a graphite layer on silver could allow to take advantage of this characteristic of carbon. The deposition of a tiny layer of graphite, 1 nm thick for instance, seems to have a very significant impact on the yield curve, since the second cross-over point is immediately divided by two. The maximum yield is also reduced, since it is close to that of carbon slightly lower than that of silver (1.5 instead of 1.7). This shows quite clearly the importance of the surface state on the issue of secondary emission. By gradually increasing the thickness of carbon, the yield curve slowly tends towards that of pure carbon (Fig. 3). The effect, however, is quite progressive. Going from 1 nm to 3 nm, i.e. multiplying the thickness of graphite by 3, hardly changes our yield curve. This tends to show that the direct impact of the graphite deposition is most certainly related to the very near surface state. To observe a more significant effect of attenuation of the TEY, it is necessary to increase the thickness of carbon up to 5 nm. We then reach the order of magnitude of the range of the secondary electrons. Between 5 nm and 10 nm the yields evolve again rather little. We can certainly associate this observation to the fact that we remain in the order of magnitude of the escape depths of the majority of secondary electrons. Most of secondary electrons have an energy in the order of 50 eV that corresponds to a range of few nanometers in carbon. The full convergence toward the TEY of carbon is reached with a carbon layer of ~20 nm. Almost all the secondaries cascade is then produced in this thickness of carbon. In that case, the silver substrate plays only a minor role on the TEY. It is as if we were testing a pure carbon sample. The simulation thus shows a significant effect of the graphite deposit on the TEY. The thickness does not need to be high for an impact on the TEY to be detected. A thickness of 5 to 10 nm shows a very significant effect.

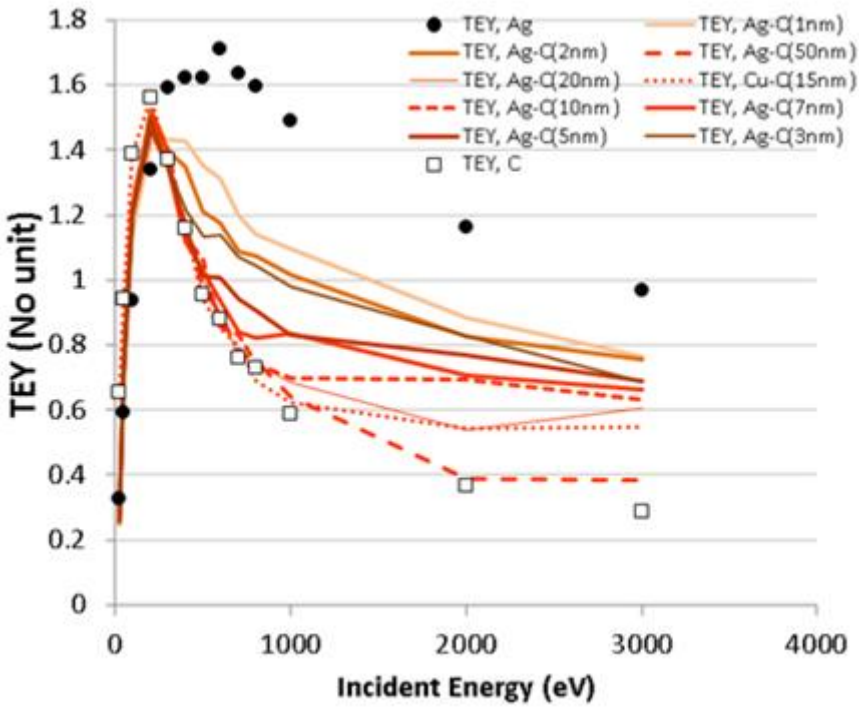

Fig. 3. TEY of a silver substrate topped with graphite thin layers having thicknesses from 1 to 50 nm. Incident electron energy is varied between 25 eV and 3 keV.

Case of copper substrate

An analogous study was carried out by considering a graphite deposit on a copper substrate. The conclusions are very similar to the previous ones obtained on a silver substrate (Fig. 3). Indeed, the energy transfers will be comparable to those of silver and the workfunction vacuum/copper of 4.7 eV is not so different from the one of silver of 4.5 eV. However, this study will allow us to draw some interesting conclusions by comparing the two substrates. With a very small deposit of 1 nm of graphite we have seen a drastic drop in the secondary emission yield of silver. The same observation is made in the case of copper, however the convergence towards the TEY of pure graphite is still less rapid. This trend must be related to the value of the energy of the secondary electrons compared to the height of the work function. This point has been investigated by studying the energy spectra of emitted electrons in different configurations.

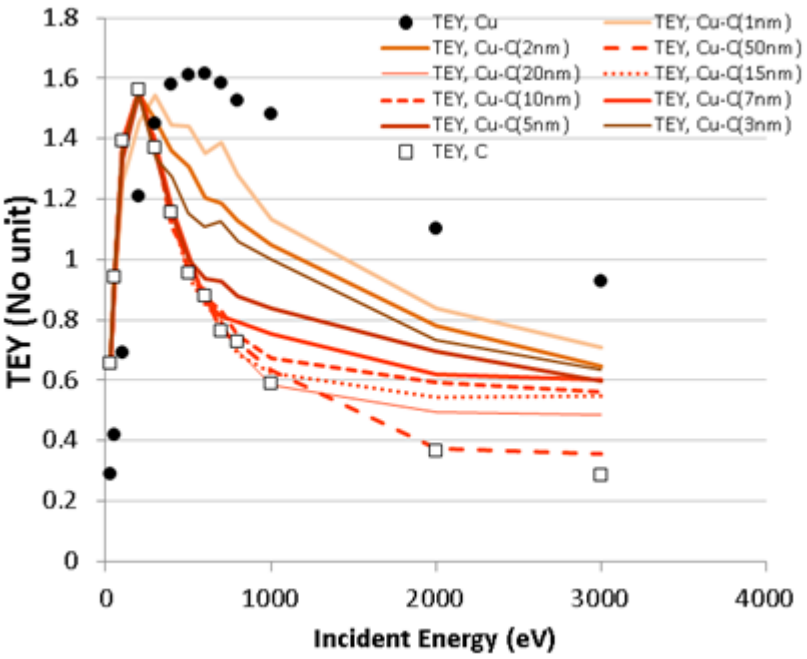

Fig. 4. TEY of a copper substrate topped with graphite thin layers having thicknesses from 1 to 50 nm. Incident electron energy is varied between 25 eV and 3 keV.

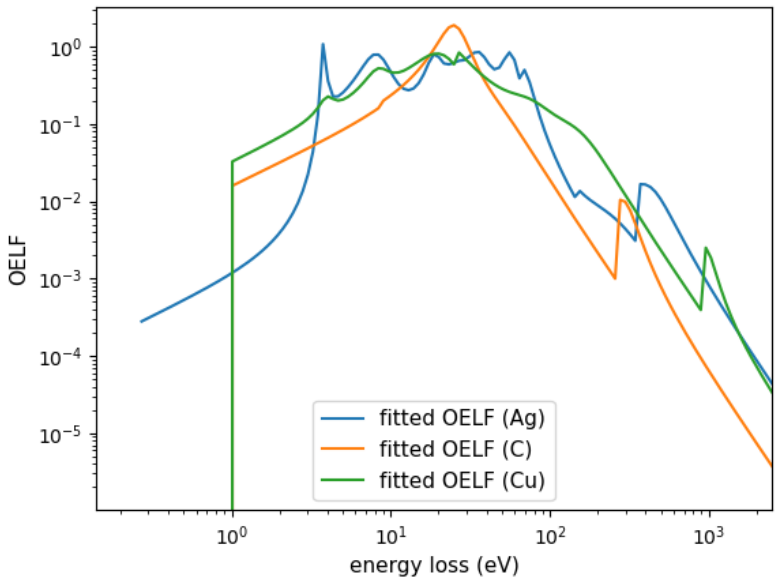

Fig. 5. Optical Energy Loss Function (OELF) of Silver, Carbon and copper substrate

The energy loss functions of the three tested materials (carbon, silver and copper) are presented in Fig. 5. This figure shows that silver will produce an important amount of very low energy electrons at the typical energy of 3.8eV, corresponding to its typical surface plasmon. A second peak can be observed at ~7 eV. Silver will thus produce an important population of very low energy electrons below ~10 eV. On the contrary Carbon will produce an important amount of secondary electrons with an energy around its typical plasmon energy of ~24 eV. Copper OELF has its maximum value around 15 eV at which a large population of secondary electrons is expected. To summarize Silver will produce less energetic secondaries than copper and carbon which should have the most energetic secondary population.

In conclusion, a change in the work function potential barrier of the vacuum/material interface will have a stronger impact in the material where the least energetic electrons are produced, i.e. silver. And this is what we observe in our simulations of secondary emission yields.

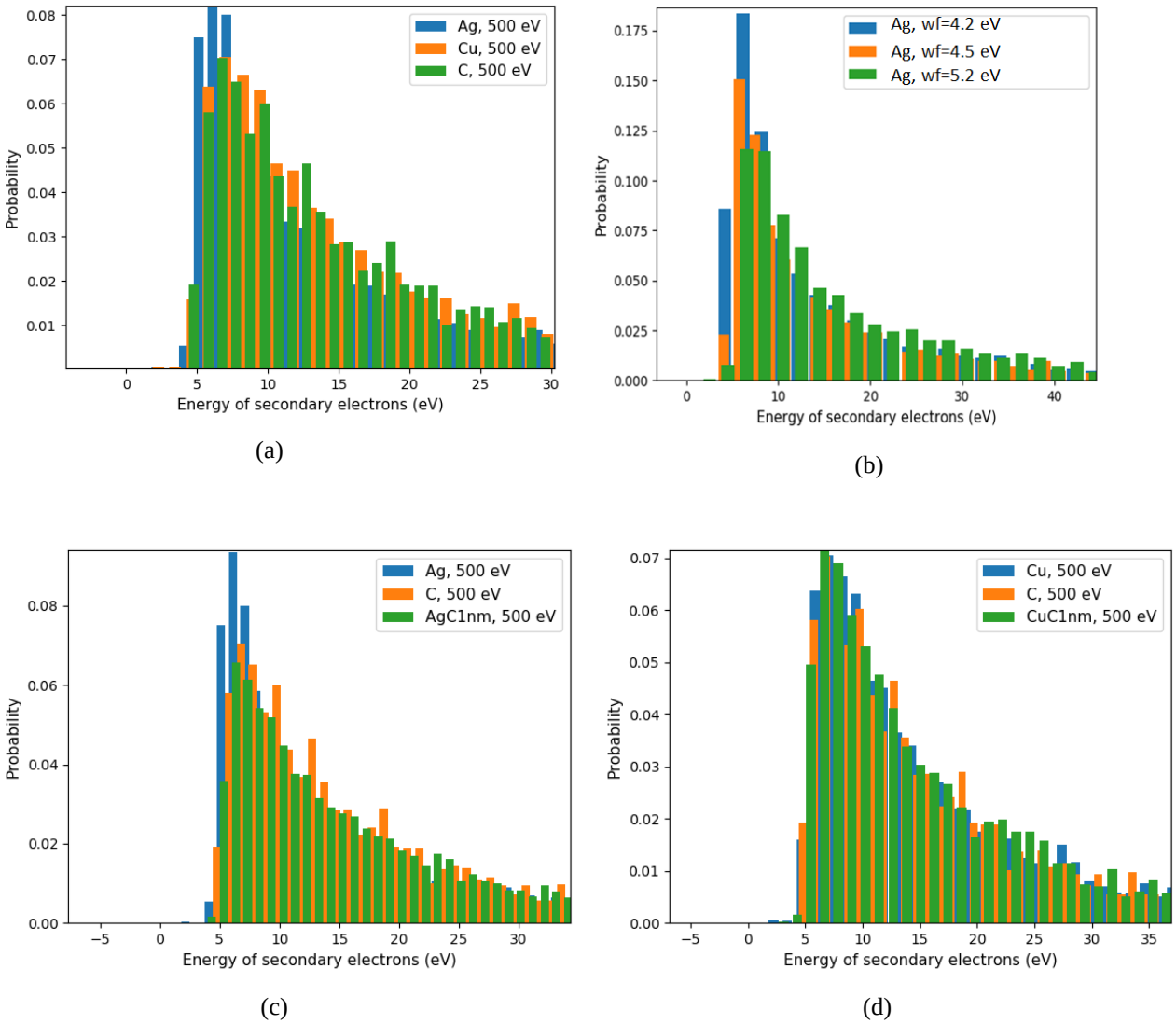

Fig. 6. Energy spectrum of low energy electrons produced by 500 eV electrons, in carbon, silver and copper (a) simulated with their standard work function values (resp.4.8 eV (C), 4.5 eV (Ag), 4.2 eV (Cu)). In silver with various work functions (4.2 eV, 4.5 eV and 5.2 eV), (b). In silver, graphite and silver topped with 1nm of graphite (c). In copper, graphite and copper topped with 1nm of graphite (c).

The analysis of energetic spectra of secondary electrons was conducted in light of the different OELF characteristics. Fig. 6 (a) shows the energetic spectra of emitted electrons at very low energy, below 30 eV, produced by 500 eV incident electrons in the three materials. The shape of the different spectra is in agreement with the OELF. Silver presents the most important population of electrons below 7 eV. In contrast, the spectra of copper and carbon are quite comparable. Energy transfer lower than the plasmon energy remains always possible leading to a thermalization process within the cascade of ionization leading to similar energetic distributions for emitted electrons. The second panel (b) of Fig. 6 depicts the impact on the spectrum of emitted electrons. One can clearly see that increasing the work function of silver, leads to a direct cut of the part of the spectrum below 7 eV. The panel (c) of the figure compares the energetic distribution of silver and carbon with the one of a sample of silver topped with 1 nm of carbon. The energetic distribution of this last case (Ag topped with C) is comparable to that of pure carbon. This shows that the electrons produced beyond 1 nm depth in the silver no longer leave the material. A part of these electrons must be stopped by the increase of the potential barrier. But this also means

that the majority of the electrons that leave the material come from the first nanometer. The last panel (d) of Fig. 6 shows similar calculations for a copper substrate.

COMPARISON WITH EXPERIMENTAL DATA

A comparison of simulated TEY of copper volumes topped with carbon layers of increasing thicknesses has been performed with experimental measurements [12]. The main results extracted from ref. [12] are reminded here. In order to improve the comparison with experimental data, the parameters of the Monte Carlo simulations have been optimized to best fit TEY of both pure Carbon and copper bulk materials. The fit of OELF has been improved for copper and the average potential energy of weakly bond electrons has also been selected for both materials in order to best fit TEY of pure materials. In this way, the behavior of the TEY curves when changing the thickness of the carbon overlayer can be closely compared to experimental measurements. The general trend observed experimentally is well reproduced by Monte Carlo simulations. A very thin layer of carbon of few nanometers is sufficient to change significantly the TEY of the copper substrate. The TEY is driven by the first ~5 nm of the surface of the material.

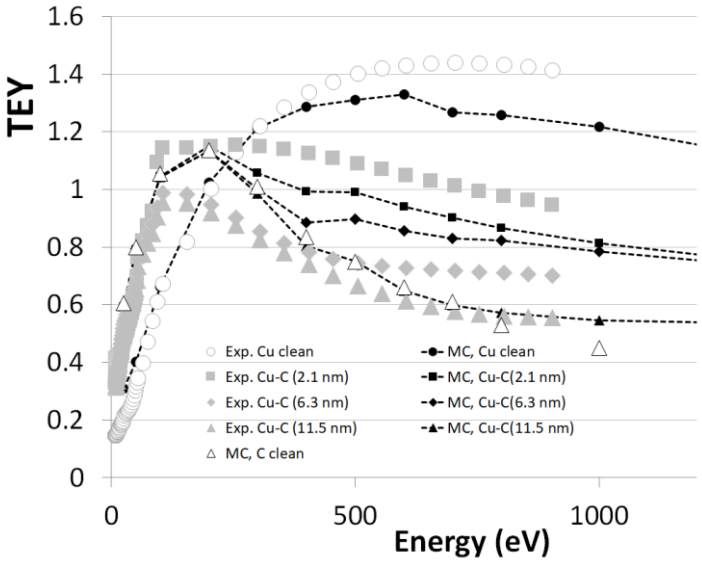

Fig. 7. Comparison with experimental data of ref. [4] of total electron emission yield (TEY) calculated for various carbon thickness layers of 2.1 nm, 6.3 nm and 11.5 nm. A very thin layer of carbon of few nanometers is sufficient to change significantly the TEY of the copper substrate.

CONCLUSION

The impact of a carbon layer covering both silver and copper substrates has been analysed. The simulations are in good agreement with experimental data, which showed that few nanometers ($\lesssim$ ~ 5 nm) of a carbon coating is enough to reduce significantly the TEY of these two materials. Beyond a thickness of 5 nm the TEY is essentially driven by the material deposited on the surface. The TEY is dominated by very low energy electrons having energy below some tens of eV. These electrons can escape the material only if they are produced close to the surface (< 5nm). The nature of the surface material has the main impact of the TEY, because the amount of low energy electrons varies strongly from a material to another. The work function height is a parameter of second importance even if its impact can be significant. In the case of copper material, an increase of the work function by some tens % leads to a decrease of the TEY in the same order of magnitude. This value can change from a material to another depending on the value of the energy of secondary electrons relatively to the height of the work function.

REFERENCES

[1] Cazaux J, 2010 J. of Elec. Spect. and Rel. Pheno. **176(1)**, 58-79

[2] Balcon N, Payan D, Belhaj M, Tondu T, and Inguimbert V 2012 IEEE Trans. Plasma Sci. **40(2)** 282-290, doi: 10.1109/TPS.2011.2172636

[3] Montero I, Aguilera L, Dávila M E, Nistor V, González L A, Galán L, Raboso D, Ferritto R, 2014 Appl. Surf. Sci. **291**, 74-77
[4] Angelucci M, Novelli A, Spallino L, Liedl A, Larciprete R, and Cimino R 2020 Phys. Rev. Research. **2**, 032030
[5] M. Raine, M. Gaillardin, P. Paillet, Geant4 physics processes for silicon microdosimetry simulation: Improvements and extension of the energy-range validity up to 10 GeV/nucleon, Nuclear Instruments and Methods in Physics Research Section B: Beam Interactions with Materials and Atoms. 325 (2014) 97–100. https://doi.org/10.1016/j.nimb.2014.01.014.
[6] J. Pierron, C. Inguimbert, M. Belhaj, T. Gineste, J. Puech, M. Raine, Electron emission yield for low energy electrons: Monte Carlo simulation and experimental comparison for Al, Ag, and Si, Journal of Applied Physics. 121 (2017) 215107. https://doi.org/10.1063/1.4984761.
[7] J. Pierron, C. Inguimbert, M. Belhaj, M. Raine, J. Puech, Ionizing Dose Calculations for Low Energy Electrons in Silicon and Aluminum, IEEE Transactions on Nuclear Science. 64 (2017) 2340–2348. https://doi.org/10.1109/TNS.2017.2662220.
[8] Q. Gibaru, C. Inguimbert, P. Caron, M. Raine, D. Lambert, J. Puech, Geant4 physics processes for microdosimetry and secondary electron emission simulation: Extension of MicroElec to very low energies and 11 materials (C, Al, Si, Ti, Ni, Cu, Ge, Ag, W, Kapton and SiO2), Nuclear Instruments and Methods in Physics Research Section B: Beam Interactions with Materials and Atoms. 487 (2021) 66–77. https://doi.org/10.1016/j.nimb.2020.11.016.
[9] H. Shinotsuka, S. Tanuma, C. J. Powell and D. R. Penn, "Calculations of electron inelastic mean free paths. X. Data for 41 elemental solids over the 50eV to 200keV range with the relativistic full Penn algorithm, "Surf. & Int.analysis, May 2015, (wileyonlinelibrary.com) DOI 10.1002/sia.5789
[10] ESTAR, https://physics.nist.gov/PhysRefData/Star/Text/ESTAR.html, National Institute of Standards and Technology, last access the 22 june 2022.
[11] F. Salvat, A. Jablonski, C.J. Powell, elsepa—Dirac partial-wave calculation of elastic scattering of electrons and positrons by atoms, positive ions and molecules, Computer Physics Communications. 165 (2005) 157–190. https://doi.org/10.1016/j.cpc.2004.09.006.
[12] J. Allison, K. Amako, J. Apostolakis, P. Arce, M. Asai, T. Aso, E. Bagli, A. Bagulya, S. Banerjee, G. Barrand, B.R. Beck, A.G. Bogdanov, D. Brandt, J.M.C. Brown, H. Burkhardt, Ph. Canal, D. Cano-Ott, S. Chauvie, K. Cho, G.A.P. Cirrone, G. Cooperman, M.A. Cortés-Giraldo, G. Cosmo, G. Cuttone, G. Depaola, L. Desorgher, X. Dong, A. Dotti, V.D. Elvira, G. Folger, Z. Francis, A. Galoyan, L. Garnier, M. Gayer, K.L. Genser, V.M. Grichine, S. Guatelli, P. Guèye, P. Gumplinger, A.S. Howard, I. Hřivnáčová, S. Hwang, S. Incerti, A. Ivanchenko, V.N. Ivanchenko, F.W. Jones, S.Y. Jun, P. Kaitaniemi, N. Karakatsanis, M. Karamitros, M. Kelsey, A. Kimura, T. Koi, H. Kurashige, A. Lechner, S.B. Lee, F. Longo, M. Maire, D. Mancusi, A. Mantero, E. Mendoza, B. Morgan, K. Murakami, T. Nikitina, L. Pandola, P. Paprocki, J. Perl, I. Petrović, M.G. Pia, W. Pokorski, J.M. Quesada, M. Raine, M.A. Reis, A. Ribon, A. Ristić Fira, F. Romano, G. Russo, G. Santin, T. Sasaki, D. Sawkey, J.I. Shin, I.I. Strakovsky, A. Taborda, S. Tanaka, B. Tomé, T. Toshito, H.N. Tran, P.R. Truscott, L. Urban, V. Uzhinsky, J.M. Verbeke, M. Verderi, B.L. Wendt, H. Wenzel, D.H. Wright, D.M. Wright, T. Yamashita, J. Yarba, H. Yoshida, Recent developments in Geant4, Nuclear Instruments and Methods in Physics Research Section A: Accelerators, Spectrometers, Detectors and Associated Equipment. 835 (2016) 186–225. https://doi.org/10.1016/j.nima.2016.06.125.
[13] C. Inguimbert , Q. Gibaru, P. Caron, M. Angelucci, L. Spallino, R. Cimino, “Modelling the impact on the secondary electron yield of carbon layers of various thicknesses on copper substrate, “ Nuc. Instr. And Meth. In Phys. Res. B 526 (2022) 1-8.